

Supporting information

Core cross-linked micelles and vesicles based on the self-assembly of double hydrophilic poly(2-oxazoline) block copolymers

Matthias Hartlieb,^{1,2} David Pretzel,^{1,2} Michael Wagner,^{1,2} Stephanie Hoepfener,^{1,2} Peter Bellstedt,³ Matthias Görlach,³ Christoph Englert,^{1,2} Kristian Kempe,^{1,2,†} Ulrich S. Schubert^{1,2,*}

¹ Laboratory of Organic and Macromolecular Chemistry (IOMC), Friedrich Schiller University Jena, Humboldtstrasse 10, 07743, Jena, Germany

² Jena Center for Soft Matter (JCSM), Friedrich Schiller University Jena, Philosophenweg 7, 07743, Jena, Germany

³ Biomolecular NMR Spectroscopy, Leibniz Institute for Age Research – Fritz Lipmann Institute, Beutenbergstr. 11, 07745 Jena, Germany

† Current address: Department of Chemistry, University of Warwick, Gibbet Hill Road, Coventry, CV4 7AL, U.K.

* Address correspondence to ulrich.schubert@uni-jena.de

I Materials and instrumentation

Chemicals and solvents were purchased from Sigma-Aldrich, Merck, Fluka, and Acros. 2-Ethyl-2-oxazoline (EtOx) and methyl tosylate (MeOTos) were distilled to dryness prior to use. EtOx was dried using barium oxide before distillation. 2-(4-((*tert*-Butoxycarbonyl)amino)butyl)-2-oxazoline (BocOx) was synthesized as described in a previous publication.¹

The Initiator Sixty single-mode microwave synthesizer from Biotage, equipped with a non-invasive IR sensor (accuracy: 2%), was used for polymerizations under microwave irradiation.

Microwave vials were heated overnight to 110 °C and allowed to cool to room temperature under argon atmosphere before use. All polymerizations were carried out under temperature control. Size-exclusion chromatography (SEC) of protected polymers was performed on a Shimadzu system equipped with a SCL-10A system controller, a LC-10AD pump, a RID-10A refractive index detector and a PSS SDV column with chloroform/triethylamine (NEt₃)/*iso*-propanol (94:4:2) as eluent. The column oven was set to 50 °C. SEC of the deprotected statistical copolymers was performed on a Shimadzu system with a LC-10AD pump, a RID-10A refractive index detector, a system controller SCL-10A, a degasser DGU-14A, and a CTO-10A column oven using *N,N*-dimethyl acetamide (DMAc) with 2.1 g L⁻¹ LiCl as the eluent and the column oven set to 50 °C. Poly(styrene) (PS) samples were used as calibration standards for both solvent systems. Proton NMR spectroscopy (¹H NMR) measurements were performed at room temperature on a Bruker AC 300 and 400 MHz spectrometer, using CDCl₃ or *N,N* dimethyl formamide (DMF)-D₇ as solvents. The chemical shifts are given in ppm relative to the signal of the residual non-deuterated solvent.

Batch dynamic light scattering (DLS) was performed on a Zetasizer Nano ZS (Malvern Instruments, Herrenberg, Germany). All measurements were performed in folded capillary cells (DTS1071, Malvern Instruments, Herrenberg, Germany). After an equilibration time of 180 s, 3 × 30 s runs were carried out at 25 °C ($\lambda = 633$ nm). The counts were detected at an angle of 173°. Each measurement was performed in triplicate. Apparent hydrodynamic radii, R_h, were calculated according to the Stokes–Einstein equation.

Laser Doppler velocimetry was used to measure the electrokinetic potential, also known as zeta potential. The measurements were performed on a Zetasizer Nano ZS (Malvern Instruments, Herrenberg, Germany) in folded capillary cells (DTS1071). For each measurement, 15 runs were

carried out using the fast-field and slow-field reversal mode at 150 V. Each experiment was performed in triplicate at 25 °C. The zeta potential (ζ) was calculated from the electrophoretic mobility (μ) according to the Henry Equation.² The Henry coefficient, $f(\kappa a)$, was calculated according to Ohshima.³

Cryo-TEM investigations were conducted with a FEI Tecnai G² 20 at 200 kV acceleration voltage. Specimens were vitrified by a Vitrobot Mark V system on Quantifoil grids (R2/2). The blotting time was 1 s with blotting force offset of 0. The amount of solution was 7 μ L. Samples were plunge frozen in liquid ethane and stored under liquid nitrogen until transferred to the Gatan cryo-holder and brought into the microscope. Images were acquired with a 4k \times 4k CCD Eagle camera.

Solid state (ss) NMR spectroscopy

One-dimensional (1D) natural abundance ¹³C cross polarization magic angle spinning ssNMR spectroscopy was carried out using a Bruker Avance II spectrometer operating at ¹H (¹³C) frequencies of 500 (125) MHz and using a 3.2 mm triple resonance probe. Sample temperature was 293 K at 20 kHz spinning frequency. Cross polarization (CP) contact time was 1.5 ms, and ¹H decoupling was performed using 90 kHz decoupling field strength. Final spectra were collected with 295006 scans and a 2 s recycle time, processed (exponential window function; line broadening 20 Hz) and evaluated with Bruker Topspin. Referencing was relative to Adamantan, setting the methine line to 29.46 ppm relative to neat trimethylsilane.⁴

Asymmetric flow field-flow fractionation (AF4)

Asymmetric flow field-flow fractionation (AF4) was performed on an AF2000 MT System (Postnova Analytics, Landsberg, Germany) coupled to an UV (PN3211, 260 nm), RI (PN3150), MALLS (PN3070, 633 nm) and DLS (ZetaSizerNano ZS, 633 nm) detector. The eluent is delivered by two different pumps (tip and focus-flow) and the sample is injected by an auto-sampler (PN5300) into the channel. The channel has a trapezoidal geometry and an overall area of 31.6 cm². The nominal height of the spacer was 500 μm and a regenerated cellulose membrane with a molar mass cut-off of 10,000 g mol⁻¹ was used as accumulation wall. All experiments were carried out at 25 °C. For molar mass determination of the polymers, the eluent was composed of 25 mM acetate buffer at a pH value of 3.5 and 20 mM NaCl. The detector flow rate was set to 0.5 mL min⁻¹ for all samples and 50 μL (5 mg mL⁻¹) were injected with an injection flow rate of 0.2 mL min⁻¹ for 7 min. For all samples the cross-flow was set to 1.8 mL min⁻¹. After the focusing period and a transition time of 1 min, the cross flow was kept constant for 3 min and then decreased under a power function gradient (0.4) to 0 within 15 min. Afterwards, the cross-flow was kept constant at zero for at least 20 min to ensure complete elution. For characterization of the colloidal structures, the eluent was 0.025% NovaChem Surfactant 100 detergents mix. The detector flow rate was set to 0.5 mL min⁻¹ for all samples and 20 μL (5 mg mL⁻¹) were injected with an injection flow rate of 0.2 mL min⁻¹ for 7 min. For all samples the cross-flow was set to 1.0 mL min⁻¹. After the focusing period and a transition time of 1 min, the cross flow was kept constant for 2 min and then decreased under a power function gradient (0.4) to 0 within 18 min. Afterwards, the cross-flow was kept constant at zero for at least 25 min to ensure complete elution. For calculation of the molar mass and the radius of gyration, a Zimm plot was used. All measurements were repeated three times. The refractive

index increment (dn/dc) of all samples was measured by manual injection of a known concentration directly into the channel without any focusing or cross-flow. The dn/dc was calculated as the average of at least three injections from the area under the RI curve (AUC_{RI}).

II Analytics of P(EtOx)-*b*-(BocOx) and P(EtOx)-*b*-(AmOx)

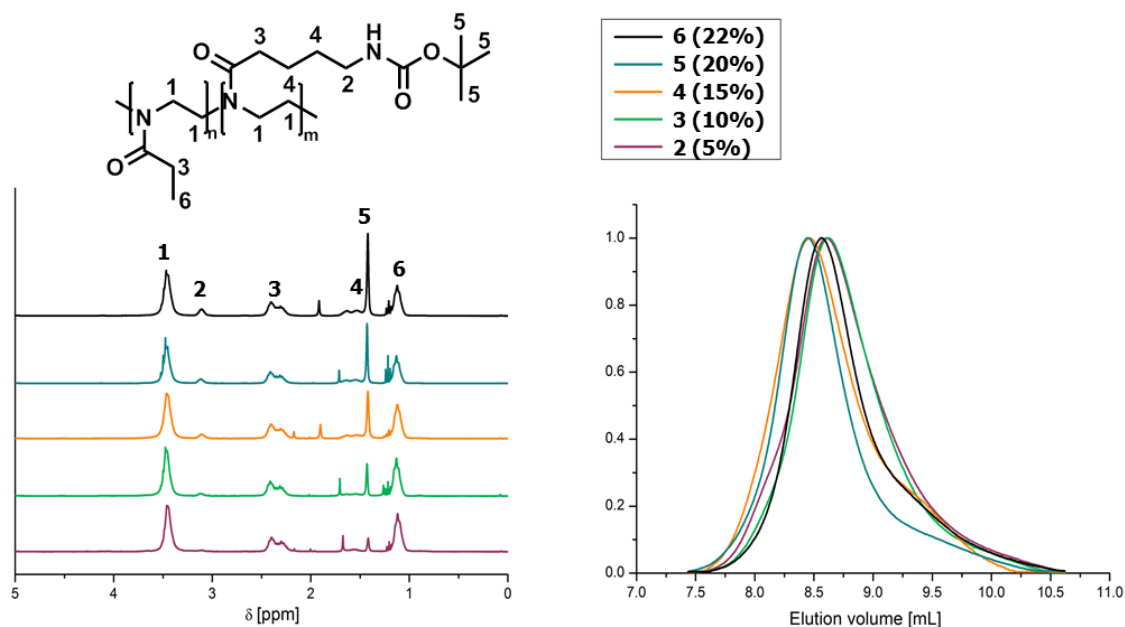


Figure S1. ^1H NMR spectra (300 MHz, CDCl_3) and size exclusion chromatograms (chloroform/ NEt_3 /*iso*-propanol) of the protected block copolymers (P(EtOx)-*b*-BocOx, **2-6**) with BocOx-contents between 5 and 22%.

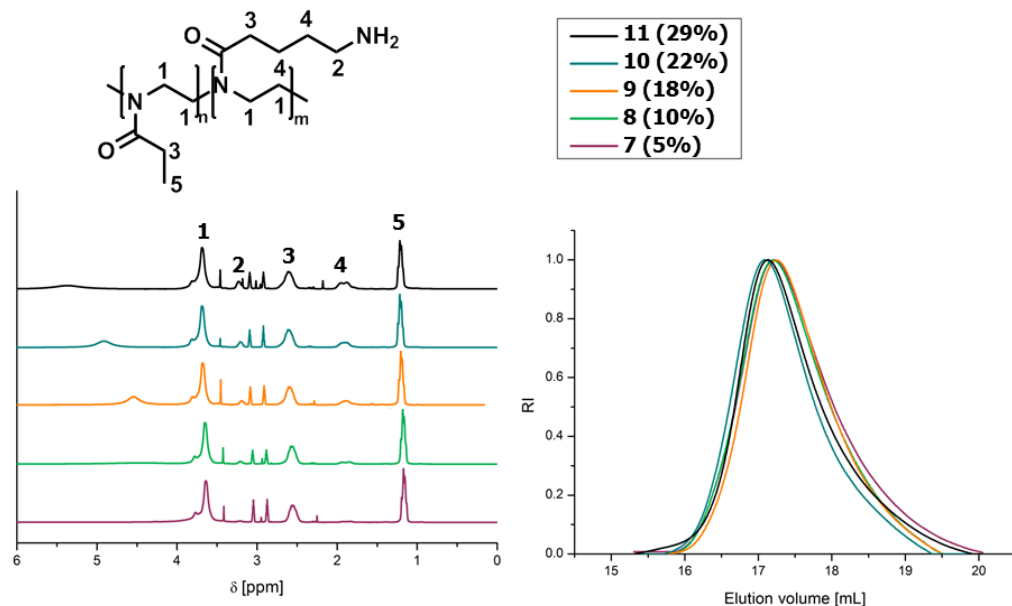


Figure S2. ^1H NMR spectra (300 MHz, DMF-D_7) and size exclusion chromatograms (N,N -dimethyl acetamide) of the deprotected block copolymers (P(EtOx-*b*-AmOx, **7-11**) with AmOx-contents between 5 and 29%.

Table S1. Asymmetric flow field flow fractionation (AF4) data of the deprotected block copolymers.

Sample	dn/dc [mL g^{-1}]	M_n [g mol^{-1}]	Error [g mol^{-1}]	M_w [g mol^{-1}]	Error [g mol^{-1}]	M_z [g mol^{-1}]	Error [g mol^{-1}]	\mathcal{D}	Error	Rec [%]	Error [%]
7	0.153	11,700	670	12,900	530	14,000	560	1.10	0.024	73.7	0.1
8	0.160	9,200	360	10,500	840	11,300	860	1.14	0.065	74.9	0.9
9	0.153	13,300	340	14,600	270	15,900	260	1.10	0.008	77.6	0.3
10	0.156	13,600	430	14,900	450	16,600	820	1.09	0.003	77.1	0.5
11	0.139	12,500	500	15,700	180	18,100	380	1.26	0.039	75.9	0.9

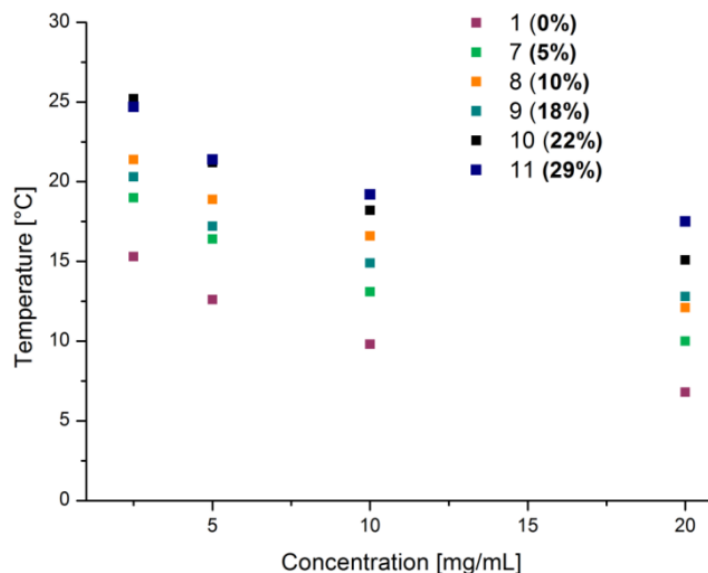


Figure S3. Cloud-points of P(EtOx-*b*-AmOx) in dependency of the concentration.

In a recent publication we described the formation of cationic hydrogels, originating from statistical copolymers P(EtOx-*stat*-AmOx) with comparable compositions, which were formed due to phase separation during the gelation leading to micron-sized hydrogel beads.⁵ Such a behavior was observed under strong alkaline conditions (5 wt% aqueous NaOH) at elevated temperatures (50 °C). As a consequence, the prepared P(EtOx-*b*-AmOx) block copolymers were investigated regarding their LCST behavior at the conditions described earlier, revealing a similar phase transition (Figure S3). However, also a PEtOx homopolymer was included into the study and exhibited a lower T_{cp} than any of the copolymers. This prompted us to conclude that PEtOx is the segment which undergoes phase separation upon heating. This can be explained by a chaotropic influence of the high hydroxyl ion concentration in solution.^{6, 7} Therefore, the phase separation at these conditions cannot be exploited to create micellar systems with the cationic building block in the core since PEtOx collapses at increasing temperatures.

III Analytics of cross-linked and non-cross-linked self-assembled structures.

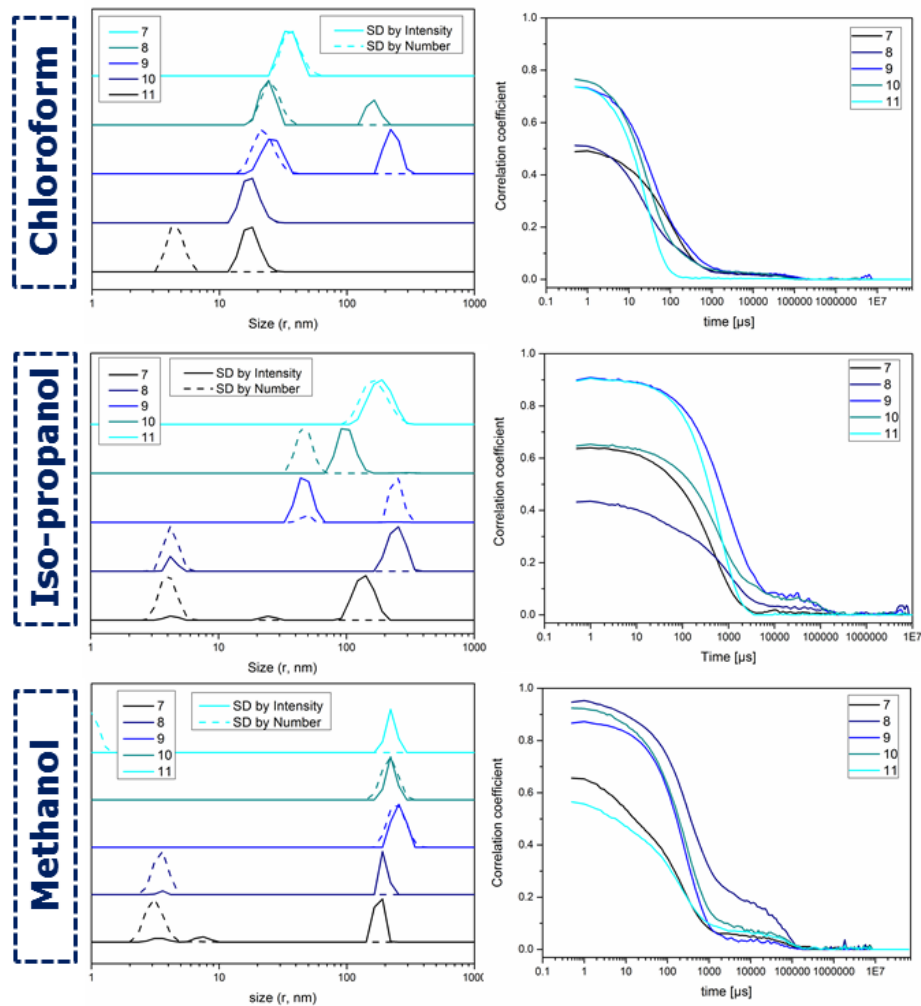


Figure S4. DLS size distributions and correlation functions of P(EtOx-*b*-AmOx) in organic solvents (1 mg mL⁻¹).

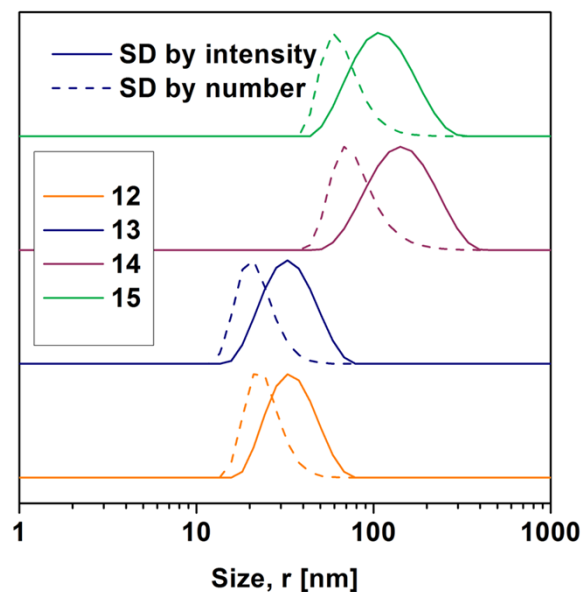


Figure S5. DLS size distributions of cross-linked nanostructures in water.

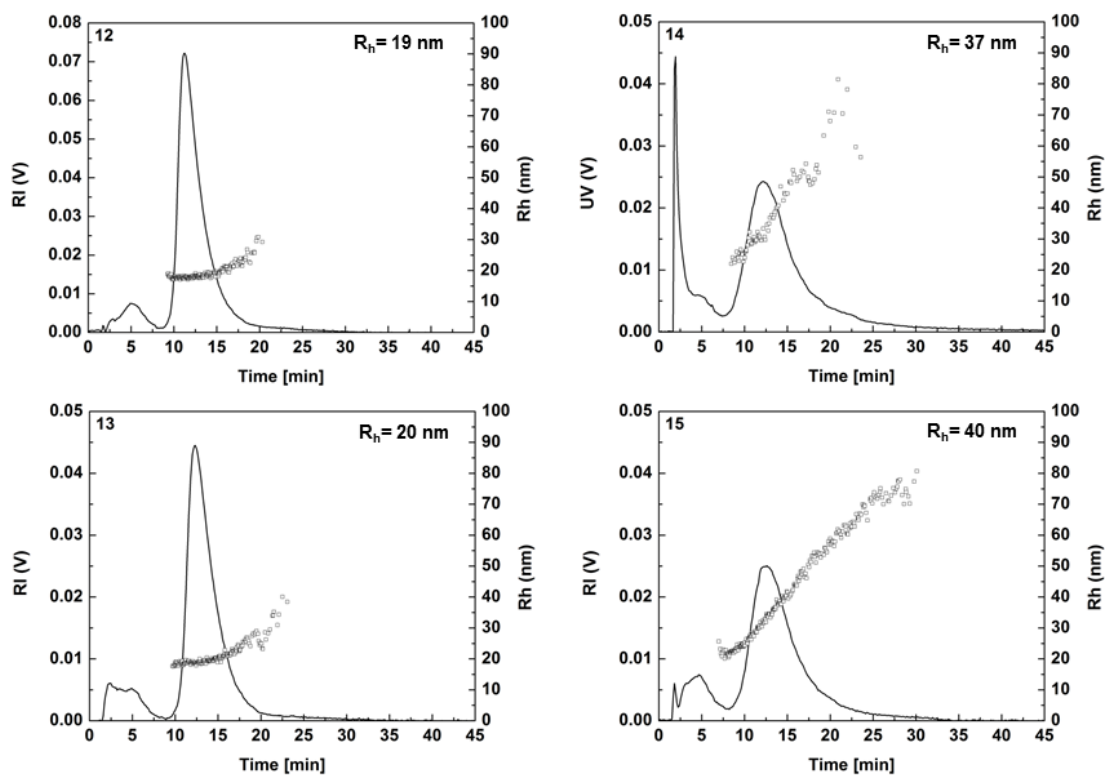


Figure S6. AF4 elugrams of cross-linked nanostructures (in 0.025% NovaChem Surfactant 100 detergents mix).

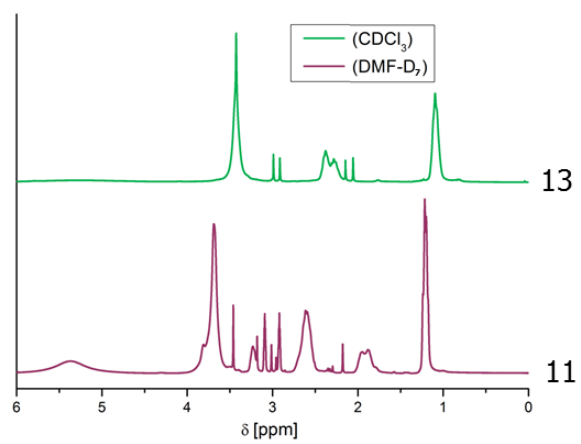


Figure S7. Comparison of the ¹H NMR spectra of polymer **11** in CDCl₃ (self-assembly) and DMF-D₇ (no assembly).

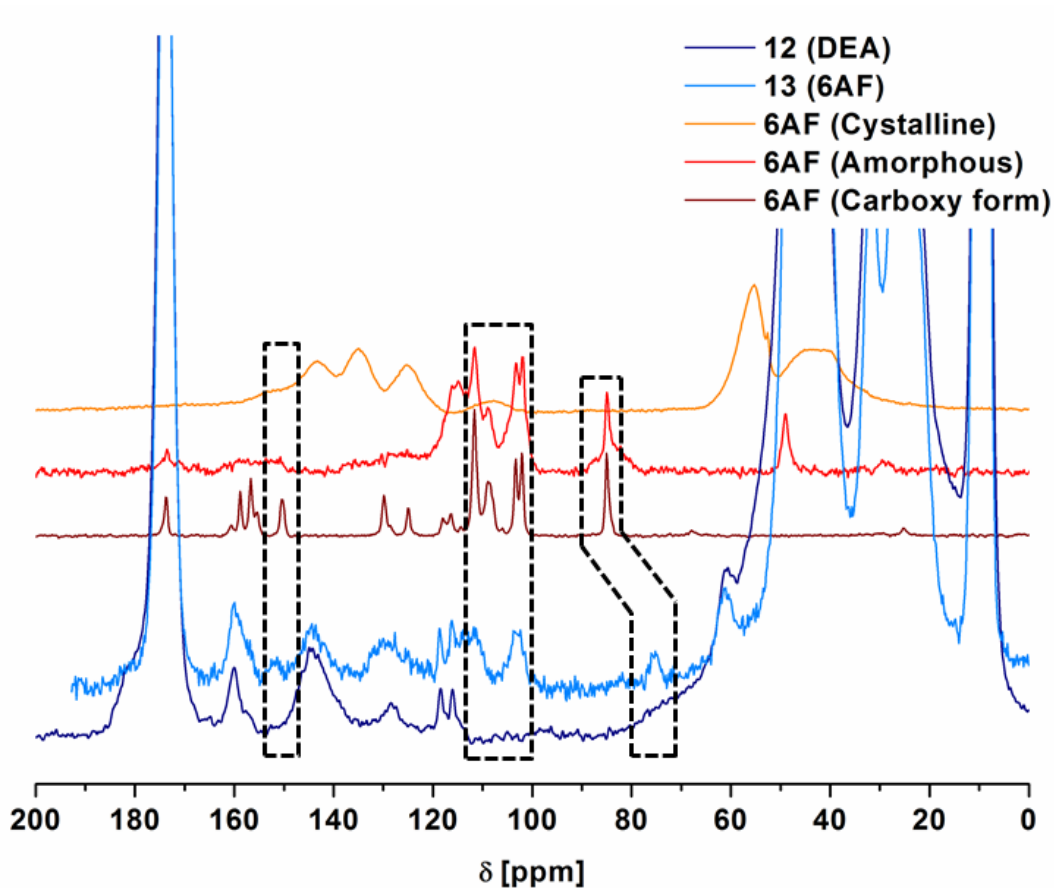


Figure S8. Solid state ^{13}C NMR spectra of different 6AF forms and micelles with (**13**) and without (**12**) 6AF. Commercial, microcrystalline 6AF, amorphous 6AF and KOH-induced ring-opened 6AF were analyzed by natural abundance ^{13}C CP MAS ssNMR. All MAS ssNMR spectra were acquired at 293 K, with 295006 scans, 2 s recycle time and a CP contact time of 1.5 ms. Microcrystalline 6AF was used as commercially supplied, amorphous 6AF was produced by dissolving commercial 6AF in MeOH, flash-freezing in liquid N_2 and subsequent lyophilisation; ring-open 6AF was derived from microcrystalline material by dissolving it in 1 M KOH, subsequent flash-freezing and lyophilisation.

IV Cellular uptake and co-localization studies of nano-assemblies.

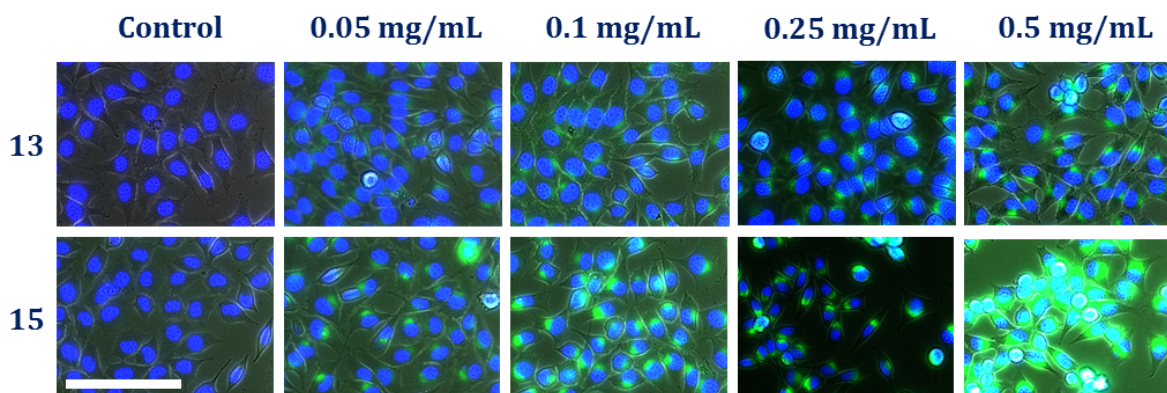


Figure S9. Fluorescence microscopy images on the concentration dependent uptake of dye containing micelles (**13**)/vesicles (**15**) by L929 mouse fibroblasts. Cells were incubated for 24 h using micelle/vesicle concentrations in the range between 0.05 and 0.5 mg mL⁻¹. Cells incubated with culture medium only served as control. The cell nuclei were stained with blue fluorescent Hoechst 33342. Shown are fluorescence images resulting from superimposing the blue and green channels. Increasing green fluorescence emitted by the dye-containing micelles/vesicles indicates a concentration dependent internalization of both structures with an elevated uptake of vesicles *vs.* micelles. Scale bar 50 μ m.

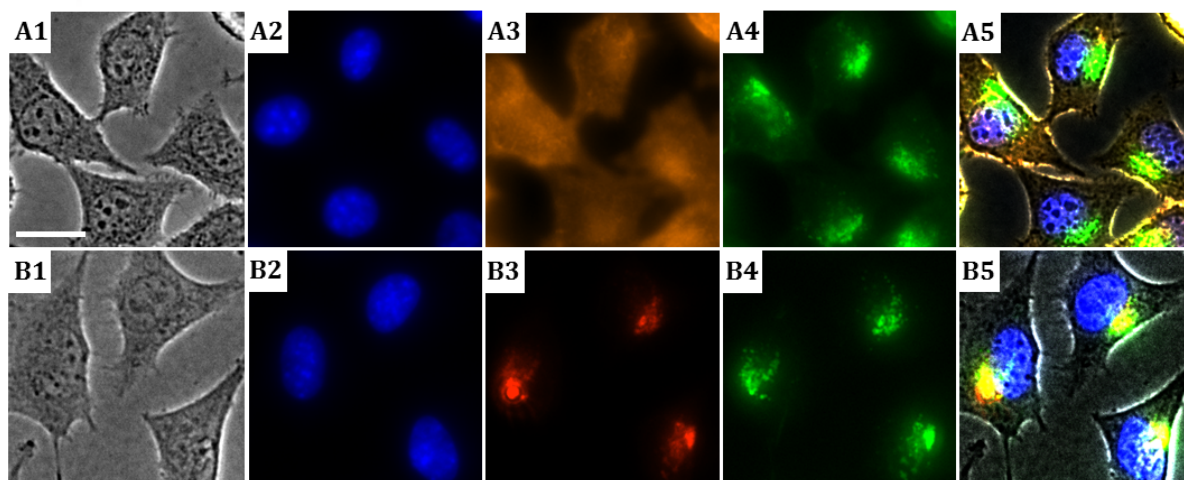


Figure S10. Representative bright field (A1 and B1) and epifluorescence images of adherent L929 cells after 24 h incubation at 37 °C in the presence of micelles (**13**) at a concentration of 0.1 mg mL⁻¹. Cell nuclei (A2 and B2), cell membranes (A3) or late endosomes/lysosomes (B3) were specifically stained and their fluorescence signal was captured in addition to the fluorescence signal originating from the internalized 6AF labeled vesicles (A4 and B4). Superimposition of all four channels (A5 and B5). Scale bar: 20 μm.

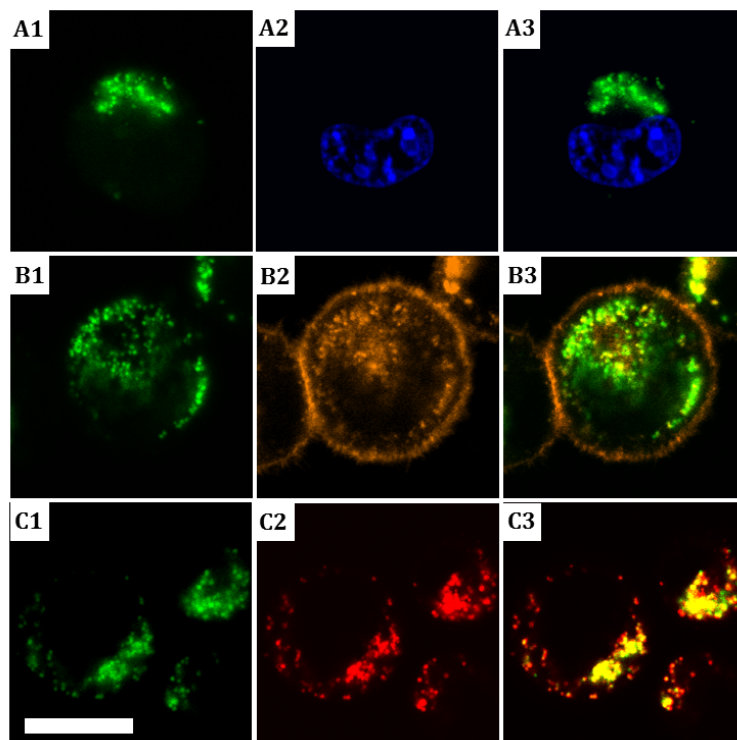


Figure S11. Representative CLSM images of detached L929 cells after 24 h incubation at 37 °C in the presence of micelles (**13**) at a concentration of 0.1 mg mL⁻¹. Cell membranes (A2), cell nuclei (B2), or late endosomes/lysosomes (C2) were specifically stained and correlated with the fluorescence signal of 6AF labeled micelles (A1, B1, and C1). Superimposition of both channels (A3, B3 and C3) proves intracellular (A3) but extra-nuclear (B3) localization of the vesicles and their apparent co-localization with lysosomal structures (C3). Scale bar: 10 μm.

References

1. M. Hartlieb, D. Pretzel, K. Kempe, C. Fritzsche, R. M. Paulus, M. Gottschaldt and U. S. Schubert, *Soft Matter*, 2013, **9**, 4693-4704.
2. A. V. Delgado, F. Gonzalez-Caballero, R. J. Hunter, L. K. Koopal and J. Lyklema, *J. Colloid Interface Sci.*, 2007, **309**, 194-224.
3. H. Ohshima, *Journal of Colloid and Interface Science*, 1994, **168**, 269-271.
4. C. R. Morcombe and K. W. Zilm, *J. Magn. Reson.*, 2003, **162**, 479-486.
5. M. Hartlieb, D. Pretzel, C. Englert, M. Hentschel, K. Kempe, M. Gottschaldt and U. S. Schubert, *Biomacromolecules*, 2014, **15**, 1970-1978.
6. M. M. Bloksma, D. J. Bakker, C. Weber, R. Hoogenboom and U. S. Schubert, *Macromol. Rapid Commun.*, 2010, **31**, 724-728.
7. F. E. Bailey and R. W. Callard, *J. Appl. Polym. Sci.*, 1959, **1**, 56-62.